*Published online 12 April 2017*

*Nucleic Acids Research, 2017, Vol. 45, No. 11* ***6471–6485***
*doi: 10.1093/nar/gkx263*

# SeqA structures behind *Escherichia coli* replication forks affect replication elongation and restart mechanisms

**Ida Benedikte Pedersen[1], Emily Helgesen[1], Ingvild Flåtten[1], Solveig Fossum-Raunehaug[1,2] and Kirsten Skarstad[1,2,*]**

[1]Department of Molecular Cell Biology and Department of Microbiology, Oslo University Hospital, P.O. Box 4950, 0424 Oslo, Norway and [2]School of Pharmacy, Faculty of Mathematics and Natural Sciences, University of Oslo, P.O. Box 4950, 0424 Oslo, Norway

Received February 01, 2016; Revised March 27, 2017; Editorial Decision March 28, 2017; Accepted April 07, 2017

## ABSTRACT

**The SeqA protein binds hemi-methylated GATC sites and forms structures that sequester newly replicated origins and trail the replication forks. Cells that lack SeqA display signs of replication fork disintegration. The broken forks could arise because of over-initiation (the launching of too many forks) or lack of dynamic SeqA structures trailing the forks. To confirm one or both of these possible mechanisms, we compared two *seqA* mutants with the *oriCm3* mutant. The *oriCm3* mutant over-initiates because of a lack of origin sequestration but has wild-type SeqA protein. Cells with nonfunctional SeqA, but not *oriCm3* mutant cells, had problems with replication elongation, were highly dependent on homologous recombination, and exhibited extensive chromosome fragmentation. The results indicate that replication forks frequently break in the absence of SeqA function and that the broken forks are rescued by homologous recombination. We suggest that SeqA may act in two ways to stabilize replication forks: (i) by enabling vital replication fork repair and restarting reactions and (ii) by preventing replication fork rear-end collisions.**

## INTRODUCTION

The single chromosome of *Escherichia coli* (*E. coli*) is replicated bi-directionally by a pair of replisomes moving in opposite directions from the origin (1). During this process, the replication forks can stall, disintegrate, or collapse if they encounter DNA damage, DNA secondary structures or tightly bound proteins (1,2). Restart mechanisms can act on a stalled fork (2–6), but a paused replisome may last a few minutes at most before falling apart (7). If replication forks disintegrate, the resulting double strand breaks (DSBs) or double strand ends (DSEs) can lead to chromosomal fragmentation (8,9). Restart and repair can depend on the recombinase RecA and involve homologous recombination (Figure 1C, ii), or be RecA independent, with digestion of the DSE by RecBCD and a direct restart (Figure 1C, iii).

A DSE can arise when the last nucleotide before a nick is replicated and the replisome can no longer find the DNA template (Figure 1A, i). Another cause of DSEs is a replisome stall that lasts long enough for the next replisome to catch up from behind and rear-end it (Figure 1A, ii). In both cases, RecA-dependent homologous recombination performs the repairs to restart the forks and maintain genomic integrity (Figure 1B). RecBCD uses helicase and nuclease activities to unwind and degrade the DNA until it reaches a Chi site, a sequence occurring about every 5 kb on the *E. coli* chromosome (10,11). RecA recruited to the Chi site forms a filament with single-stranded DNA and invades an intact homologous DNA molecule. Primosomal proteins recognize the resulting DNA structures and can restart replication forks outside of *oriC* (12,13).

The replication fork reversal (RFR) model (Figure 1C) (14,15) offers a mechanism for how a stalled or disintegrated replisome can be restarted independently of RecA. Reversal of the replication fork occurs when the newly synthesized leading and lagging strands anneal, forming a Holliday junction (HJ) (Figure 1C, i). A replication fork stalled at a leading strand lesion can undergo RFR catalyzed either by RecA or RecG (13). If the reversed fork structure cannot be processed properly, RuvABC may cleave it (Figure 1C, i, right panel). In the RFR model, fork regression, possibly stimulated by RecG (16), can continue to a Chi site where RecA is loaded and recombination occurs (Figure 1C, ii). Alternatively, RecBCD can digest the DSE that is formed in the regression and displace the stabilizing RuvABC (Figure 1C, iii). Both pathways allow PriA-mediated restart of the replication fork (see (5) for a review).

*To whom correspondence should be addressed. Tel: +47 23071186; Fax: +47 23074061; Email: Kirsten.Skarstad@rr-research.no

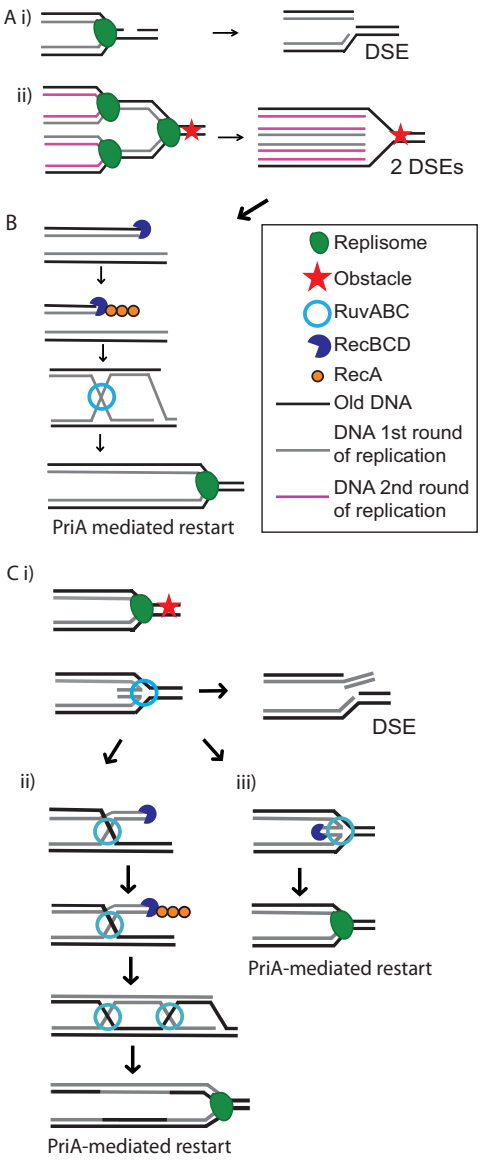


**Figure 1.** Examples of causes of DSEs at replication forks and models for repair and restart of replication forks. (**A**, i) A nick in the template DNA may cause a DSE when the replisome runs into it and (ii) rear-ending causes two DSEs when the replisomes replicate the final nucleotides of the template DNA that was replicated in the previous round. (**B**) DSEs are repaired by homologous recombination. RecBCD recognizes the DSE and unwinds and degrades the DNA up to the nearest Chi site (10,11). Next, RecA forms a filament with single-stranded DNA from the processed DSE, invades the intact homologous DNA, and performs recombination. The resulting Holliday junction is resolved by RuvABC, and PriA can restart the replication fork (12,13). (**C**, i) The replication fork encounters an obstacle/lesion and regresses. The newly synthesized leading and lagging strands anneal in this reaction, which creates a DSE. Under normal circumstances, the reversed fork structure can be resolved and restarted with or without the involvement of RecA (reviewed in (4,5)). (ii) In the RecA-dependent pathway, homologous recombination occurs, leading to two Holliday junctions, which are resolved by RuvABC. (iii) In the RecA-independent reaction, the DSE is digested by RecBCD, and the fork is restarted directly by PriA. However, if the reversed fork structure cannot be processed properly, the result may be cleavage of the fork by RuvABC, causing a DSE (C, i) right panel).

The *E. coli* SeqA protein was first recognized as an essential factor in origin sequestration (17–20), which inhibits origin re-initiation and helps to ensure only a single initiation per cell cycle (21–23). In *E. coli*, the newly replicated DNA is transiently hemi-methylated before Dam methylase acts on GATC sites on the new DNA strand (17). GATC sites occur at high density in the origin (*oriC*), where SeqA protein interacts with them to prevent re-initiation for about one third of the cell cycle (24–27). This sequestration period is reduced to a minimum in SeqA mutants (28).

Evidence suggests other roles for SeqA. It binds to hemi-methylated GATC sites trailing replication forks (24,27,29–34), and most cellular SeqA appears to be associated with newly replicated DNA in complexes following the fork (32,35). The fork-trailing SeqA structures likely also contain *oriC* DNA throughout the sequestration period (36) and represent a type of hyperstructure of newly replicated DNA from both forks in addition to *oriC* DNA. Recent work has identified two dynamic SeqA structures held in close proximity (less than 30 nm apart) behind the replication fork, bound to ∼100 kb of DNA on each sister molecule. The distance from these SeqA structures to the replisome has been estimated to be 200–300 nm (37). One possible interpretation is that the DNA between the dual SeqA structures and the replisome might benefit from some additional stability during processes such as recombination and DNA repair. In addition, deletion of *seqA* results in genomic fragmentation in the absence of functional RecBCD (38–40), and many of the replication forks initiated at *oriC* in these deletion mutants do not reach the terminus (40).

Together, these findings suggest that SeqA structures associated with replication forks may serve as DNA stabilizers and help prevent DSB formation during replication and/or rescue of stalled replication forks. One possibility is that SeqA supports fork restart (Figure 2A), and another is that it creates a barrier that prevents collisions between new and old forks (rear-ending) (Figure 2B). To assess the possible roles of SeqA complexes behind the replication fork, we used two *seqA* mutants, *seqA2* and *seqA4* (18,20,41,42), and compared them to cells expressing functional SeqA protein but unable to exhibit sequestration (43).

## MATERIALS AND METHODS

### Bacterial strains and growth conditions

All strains used are *E. coli* K-12 and are listed in Table 1. Cells were grown at the specified temperature (37°C or 42°C) in LB medium (LB) (10 g Tryptone, 5 g NaCl, 250 μl 4 M NaOH/l), AB minimal medium (44) supplemented with 10 μg/ml thiamine, and either 0.2% glucose and 0.5% casamino acids (glucose–CAA medium), or 0.2% glucose (glucose medium). The strain IBP05 was made by amplifying the chloramphenicol gene with the primers 5′GCG CTAAGAACCATCATTGGCTGTTAAAACATTATTA AAAATGTCAATGGCATATGAATATCCTCCTTAG and 5′CGATTTTTAGCAGACTGATATTTTCACTAAT GACTTATTTTCTGCTTACCCTGGAGCTGCTTCGA AGTTCC containing regions homologous to a region in close proximity to *oriC* and insertion of this fragment into the chromosome, as described in (45). All other strains constructed for this work were made by P1 transduction

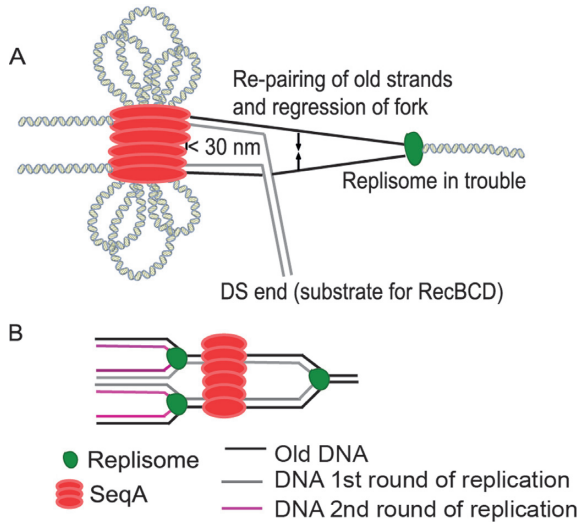


**Figure 2.** Models of how SeqA may protect the integrity of the replication fork. (**A**) Schematic illustration showing the SeqA complexes (in red) bound behind the replisome (in green) at a considerable distance (37). The bound SeqA complexes are in close proximity to each other, which means that the sister DNA is held close together behind the fork. This association could potentially provide stabilization during processes such as recombination, repair, and restart of replication forks, as illustrated here by replication fork reversal. (**B**) Stabilization of the newly replicated DNA by SeqA may create a barrier of bound protein that delays forks replicating a second round and prevents rear-ending, i.e. replication to the end of the new DNA from the first fork.

(46), as indicated in Table 1. The *recBC* Ts mutations were verified by their sensitivity to UV irradiation, but the *seqA2* and *seqA4* mutants were verified by sequencing due to a rather low co-transduction of the resistance marker gene and the mutation. The *oriCm3* mutants were verified by their asynchronous phenotype as determined by flow cytometry.

### Preparation of DNA in agarose plugs for pulsed field gel electrophoresis

Overnight cultures of *recBC* (Ts) strains at 22°C (permissive temperature) were diluted to an optical density ($OD_{600}$) of 0.005 and grown at 42°C (non-permissive temperature) in LB media to $OD_{600}$ 0.15 (exponential phase). A volume of culture corresponding to about $2.5 \times 10^8$ cells (Coulter Counter Multisizer, Beckman) was centrifuged and resuspended twice in Tris/NaCl (10 mM Tris–HCl, pH 7.6, 1 M NaCl) (initially 1 ml). Equal amounts of cell suspension (resuspended in Tris/NaCl) and molten clean-cut agarose (Bio-Rad) were brought to 42°C and combined. A total of 90 μl of the agarose/cell suspension was dispensed to wells of disposable molds (Bio-Rad), solidified, expelled into a 50 ml tube containing 2.5 ml EC lysis buffer (6 mM Tris–HCl, pH 7.6, 1 M NaCl, 100 mM EDTA, adjusted to pH 7.6 with NaOH, 1% *N*-lauryl sarcosine, 1 mg/ml lysozyme and 20 μg/ml RNase A), and incubated overnight at 37°C. After removal of the EC lysis buffer, the plugs were rinsed with TE buffer (10 mM Tris–HCl, pH 8.0, 1 mM EDTA, pH 8.0) and 2.5 ml ESP buffer was added (500 mM EDTA (adjusted to pH 9–9.5 with NaOH), 1% *N*-lauryl sarcosine, proteinase K (50 μg/ml)), followed by incubation at 37°C overnight (or 48–72 h). The plugs were then washed with TE buffer at 25°C, with three washes of 2 h each using 30 ml TE buffer. The steps above were taken from a standard protocol for preparation of plugs for pulsed field gel electrophoresis (PFGE) of bacterial DNA (47).

### CHEF-DR III PFGE and quantification

A CHEF-DR III Pulsed Field Electrophoresis system (Bio-Rad) was used to resolve the DNA. The run time was set to 21 h; temperature was 14°C; the initial and final switch times were 60 and 120 s, respectively; volts/cm was set to 6; the included angle was 120; and 0.5 × TBE was used as the running buffer. The gel was then stained with SYBR Gold Nucleic Acid Gel Stain (Life Technologies) and quantified using Genetool (Syngene) software with the rolling disc method for background subtraction. SYBR Gold Nucleic Acid Gel Stain (Life Technologies) gives a linear relationship between fluorescence intensity and DNA content over at least two orders of magnitude (48), as also applied previously (49). The percentage of chromosomal fragmentation was found by first measuring the DNA present in the well and directly beneath the well (non-fragmented DNA and most likely chromosomes with a single nick, respectively) and then measuring the DNA in the rest of the lane. The fragmented DNA value was then divided by the total DNA value. Quantification of the chromosomal fragmentation of a *rep recBC* mutant with this method was in agreement with already published results (~50%) (14).

### Flow cytometry and interpretation of DNA histograms

Cells were grown exponentially for several generations to ensure balanced growth. At an OD of 0.15, exponentially growing cells were either harvested directly or treated with rifampicin (300 μg/ml) and cephalexin (10 μg/ml) for the time equivalent of three to four generations before harvesting. Both directly harvested and treated cells were resuspended in TE buffer (10 mM Tris–HCl, pH 8.0, 1 mM EDTA, pH 8.0) and fixed in 70% ethanol. Fluorescein isothiocyanate (FITC, Sigma-Aldrich) (50) was used for protein staining (representing mass), and Hoechst 33258 was used for DNA staining (Sigma-Aldrich) (51). Flow cytometry was performed with a LSR-II flow cytometer equipped with a 488 nm argon ion laser and a 355 nm krypton laser (BD Biosciences), and the results were analyzed using FlowJo software (Tree Star, Inc.).

Rifampicin and cephalexin inhibit initiation of replication and cell division, respectively. Cells cannot initiate a new round of replication after these drugs are added but can complete ongoing rounds of replication (without dividing). DNA histograms of the treated cells thus give an integer number of chromosomes per cell with values $2^n$ or $2^{n+1}$, where $n = 0, 1, 2, 3\ldots$ represents the generation in which initiation occurs. However, this pattern holds true only for cells with synchronous initiation of replication (all origins firing simultaneously) and successful completion of replication elongation (all initiated forks reaching the terminus). DNA histograms of cells that exhibit asynchronous initiations will also contain irregular numbers of chromosomes (such as 3, 5, 7, etc.), and problems with replication elon-

**Table 1.** Strains

| Strain | Relevant features | Source |
|---|---|---|
| MG1655 | Wild type | (80,81) |
| AB1157 | Wild type | (82) |
| MG1655*oriCm3* | *oriCm3* | (43) |
| IBP05 | *oriCm3*cam | This work |
| UF340 | *seqA2* | (20) |
| UF301 | *seqA4 dam13* | (20) |
| CAG18433 | *asnB3057::Tn10* | (83) |
| SF169 | UF301 *asnB3057::Tn10* | UF301 x P1 CAG18433 |
| N1331 | Wild type | (84) |
| N1332 | *recA* Ts | (80,81,84) |
| NL40 | DS941*dif*Δ6::KmR | (85) |
| DS984 | DS941*xerC*::mini-Mu CmR | (86) |
| DS9008 | DS941*xerD*::mini-Tn10(-9) | (87) |
| SS1211 | *Δrep*::cam | (63) |
| IBP36 | MG1655 *oriCm3* | MG1655 x P1 IBP05 (this work) |
| IBP37 | MG1655 *seqA2* | MG1655 x P1 UF340 (this work) |
| IBP38 | MG1655 *seqA4* | MG1655 x P1 SF169 (this work) |
| SK129 | *recB270* (Ts) *recC271* (Ts) | (53) |
| IBP04 | SK129 *oriCm3* | SK129 x P1 IBP05 (this work) |
| IBP01 | SK129 *seqA2* | SK129 x P1 UF340 (this work) |
| IBP03 | SK129 *seqA4* | SK129 x P1 SF169 (this work) |
| ER89 | SK129 Δ*seqA21* | (39) |
| IBP07 | N1332 *oriCm3* | N1332 x P1 IBP05 (this work) |
| IBP02 | N1332 *seqA2* | N1332 x P1 UF340 (this work) |
| IBP06 | N1332 *seqA4* | N1332 x P1 SF169 (this work) |
| IBP24 | N1332 *Δrep*::cam | N1332 x P1 SS1211 (this work) |
| IBP39 | MG1655 *Δrep*::cam | MG1655 x P1 SS1211 (this work) |
| IBP40 | MG1655 *seqA2 Δrep*::cam | IBP37 x P1 SS1211 (this work) |
| IBP41 | MG1655 *seqA4 Δrep*::cam | IBP38 x P1 SS1211 (this work) |
| IBP98 | MG1655 *oriCm3 Δrep*::cam | MG1655*oriCm3* x P1 SS1211 (this work) |
| IF01 | *recA938*::cam | (88) |
| IBP87 | MG1655 *recA938*::cam | MG1655 x P1 IF01 (this work) |
| IBP80 | MG1655 *seqA2 recA938*::cam | IBP37 x P1 IF01 (this work) |
| IBP81 | MG1655 *seqA4 recA938*::cam | IBP38 x P1 IF01 (this work) |
| IBP100 | MG1655 *oriCm3 recA938*::cam | MG1655*oriCm3* x P1 IF01 (this work) |
| IBP88 | MG1655 *dif*Δ6::KmR | MG1655 x P1 NL40 (this work) |
| IBP85 | MG1655 *seqA2 dif*Δ6::KmR | IBP37 x P1 NL40 (this work) |
| IBP82 | MG1655 *seqA4 dif*Δ6::KmR | IBP38 x P1 NL40 (this work) |
| IBP101 | MG1655 *oriCm3 dif*Δ6::KmR | MG1655*oriCm3* x P1 NL40 (this work) |
| IBP89 | MG1655 *xerC*::mini-Mu CmR | MG1655 x P1 DS984 (this work) |
| IBP74 | MG1655 *seqA2 xerC*::mini-Mu CmR | IBP37 x P1 DS984 (this work) |
| IBP83 | MG1655 *seqA4 xerC*::mini-Mu CmR | IBP38 x P1 DS984 (this work) |
| IBP90 | MG1655 *xerD*::mini-Tn10(-9) | MG1655 x P1 DS9008 (this work) |
| IBP68 | MG1655 *seqA2 xerD*::mini-Tn10(-9) | IBP37 x P1DS9008 (this work) |
| IBP84 | MG1655 *seqA4 xerD*::mini-Tn10(-9) | IBP38 x P1 DS9008 (this work) |
| SMR14323 | MG1655 *ΔaraBAD567 Δattλ::PBAD zfd2509.2::PN25tetR FRTKanFRT* | (70) |
| SMR13957 | MG1655 *Δattλ::PN25tetR FRT ΔattλTn7::FRTcatFRT PN25tetO gam-GFP* | (70) |
| EH137 | MG1655 *PN25tetR PN25tetO gam-GFP* | MG1655 x P1 SMR14323 x P1 SMR13957 (this work) |
| EH138 | MG1655 *seqA2 PN25tetR PN25tetO gam-gfp* | IBP37 x P1 SMR14323 x P1 SMR13957 (this work) |
| EH139 | MG1655 *seqA4 PN25tetR PN25tetO gam-gfp* | IBP38 x P1 SMR14323 x P1 SMR13957 (this work) |

gation will be seen as a lack of distinct peaks in the 'run-out' DNA histograms (i.e. histograms of cells treated with rifampicin and cephalexin).

### Replication run-out in the absence of RecA function

Cultures of cells growing exponentially (to OD ∼0.15) at 30°C were split, and rifampicin (450 μg/ml) and cephalexin (10 μg/ml) both were added to each culture. One portion was kept at the permissive temperature (30°C) whereas the other was shifted to the non-permissive temperature (42°C) for loss of RecA function. Cells were harvested before drug treatment and after 3–4 generation times in the presence of the drugs and fixed for analysis with flow cytometry to compare replication fork run-out at each temperature. The flow histograms were analyzed using FlowJo (Tree Star, Inc.) software. The average per-cell decrease in the number of chromosomes was obtained by first identifying the number of cells in each chromosome peak, multiplying that value by each chromosome number to obtain the total number of chromosomes, and in turn dividing that by the total number of cells counted. A total of 50 000 cells were

counted for a proper estimate of the average number of chromosomes/cell. Finally, the total number of chromosomes was compared at the permissive and non-permissive temperatures.

### Viability tests

Overnight cultures were serially diluted with growth medium or 1% NaCl to approximately the same OD. A total of 5 μl of dilutions ranging from $10^{-2}$ to $10^{-6}$ were spotted onto agar plates (agar type indicated in figures).

### Gam-GFP induction, fluorescence microscopy imaging and flow cytometry of GFP

The cells were grown to OD ∼0.15 before Gam-GFP was induced by adding 10 ng/ml anhydrotetracycline. Growth was continued for 60 min, at which time the cells were immobilized on a 17 × 28 mm agarose pad (1% containing phosphate-buffered saline (PBS) with 10 ng/ml anhydrotetracycline) and covered with a no. 1.5 coverslip. Images were acquired with a Leica DM6000 microscope equipped with a Leica EL6000 metal halide lamp and a Hamamatsu ImagEM 1k camera. Phase-contrast imaging was performed with an HCX PL APO 100 × /1.40 NA objective. Fluorescence imaging was done using narrow band-pass (BP) filter sets (excitation at BP 470/40 and emission at BP 525/50 for GFP).

In the fluorescence microscopy experiments, care was taken to use the exact same settings for GFP-imaging of wild-type and *seqA* mutant cells (e.g. the same intensity, exposure time) to avoid misinterpretation. Using the publicly available ImageJ software, in post processing, we adjusted only brightness/contrast, doing so with the exact same cut-off values for images of the *seqA* mutants and wild-type cells.

Flow cytometry of Gam-GFP was performed with Accuri C6 (BD Biosciences), and the results were analyzed using FlowJo software (Tree Star, Inc.). Cells were grown as described above in glucose-CAA medium with 60-min induction of Gam-GFP (10 ng/ml anhydrotetracycline), harvested and washed in PBS directly prior to analysis with flow cytometry. A total of 50 000 cells were recorded per sample.

### Fluorescence microscopy of nucleoids

Nucleoids of fixed cells were stained with Hoechst 33258 and visualized with fluorescence microscopy, as described in (52).

## RESULTS

### Some replication forks do not reach the terminus in *seqA2* and *seqA4* mutants

In light of the chromosomal fragmentation (40) and induction of the SOS response (18) reported for *seqA* deletion strains, we used the *seqA2* and *seqA4* mutants to elucidate in more detail the importance of SeqA in stabilizing the replication fork. The *seqA2* point mutation leads to a change (N152D) in the C-terminus, resulting in a DNA binding deficiency (41), while the *seqA4* point mutation leads to a change (A25T) in the N-terminus, inhibiting multimerization (42). Thus, neither strain can form SeqA complexes on newly replicated DNA behind the replication forks.

These strains also cannot sequester *oriC* from unscheduled, premature initiations and they therefore exhibit an asynchrony phenotype (41,42). An increased number of replication forks per chromosome, as in *seqA* mutants, could lead to collisions of new and old forks (the so-called replication fork rear-ending scenario; see Figure 1A, ii). To differentiate the two causes of genomic instability—i.e. no sequestration versus having no functional SeqA behind the replication forks—our control was the *oriCm3* mutant, which lacks sequestration because of eight mutations that inactivate critical *oriC* GATC sites but has a fully functional SeqA protein (43). In these cells, extra initiations are allowed, but all cellular proteins are normal.

We use flow cytometry to investigate the DNA content and degree of asynchrony in the three mutants (Figure 3). The mean cellular DNA content was somewhat higher in the two *seqA* mutants compared to the *oriCm3* mutant (Figure 3, left panels; Table 2), but because they also had increased mass, the DNA concentration (DNA/mass) was similar to that of the *oriCm3* mutant (Table 2). Compared to the wild type, which has two peaks respectively corresponding to four and eight fully replicated chromosomes, all three mutants had an abundance of additional chromosome peaks, ranging from 3 to about 20 chromosomes. However, the run-out histogram of the *oriCm3* differed markedly from that of the two *seqA* mutants. The peaks of the *seqA* mutants were much less distinct than for the *oriCm3* mutant (Figure 3, middle panels), indicating that some replication forks could not reach the terminus during rifampicin and cephalexin incubation, presumably because of problems during fork elongation.

In addition, on microscopy analysis, the *seqA* mutants showed filamentous cells with unsegregated DNA, but the *oriCm3* mutant did not (Figure 3, right panel). The *seqA* mutants also showed a greater heterogeneity in size/mass distribution in FITC histograms from flow cytometry (Table 2). The doubling time of the two *seqA* mutants was increased ∼20% compared to wild-type cells, but the *oriCm3* mutation did not affect growth rate (Table 2). This increase in doubling time may reflect some cell death or at least a cell division delay among the *seqA* mutants (based on flow cytometry and microscopy) caused by the SOS response. The SOS response and abortion of replication forks seen here for the two *seqA* mutants are in agreement with previously reported phenotypes for SeqA-less cells (18,38,40).

The *seqA2* mutant cells seemed to show greater problems with DNA segregation and cell division compared to the *seqA4* cells, based on nucleoids under microscopy (Figure 3) and cell mass values (Table 2).

### The *seqA2* and *seqA4* mutants exhibit a significantly higher degree of chromosomal fragmentation compared to the *oriCm3* mutant

To address whether replication fork disintegration might be why forks in the *seqA* mutants do not reach the terminus, we investigated the degree of chromosomal fragmentation

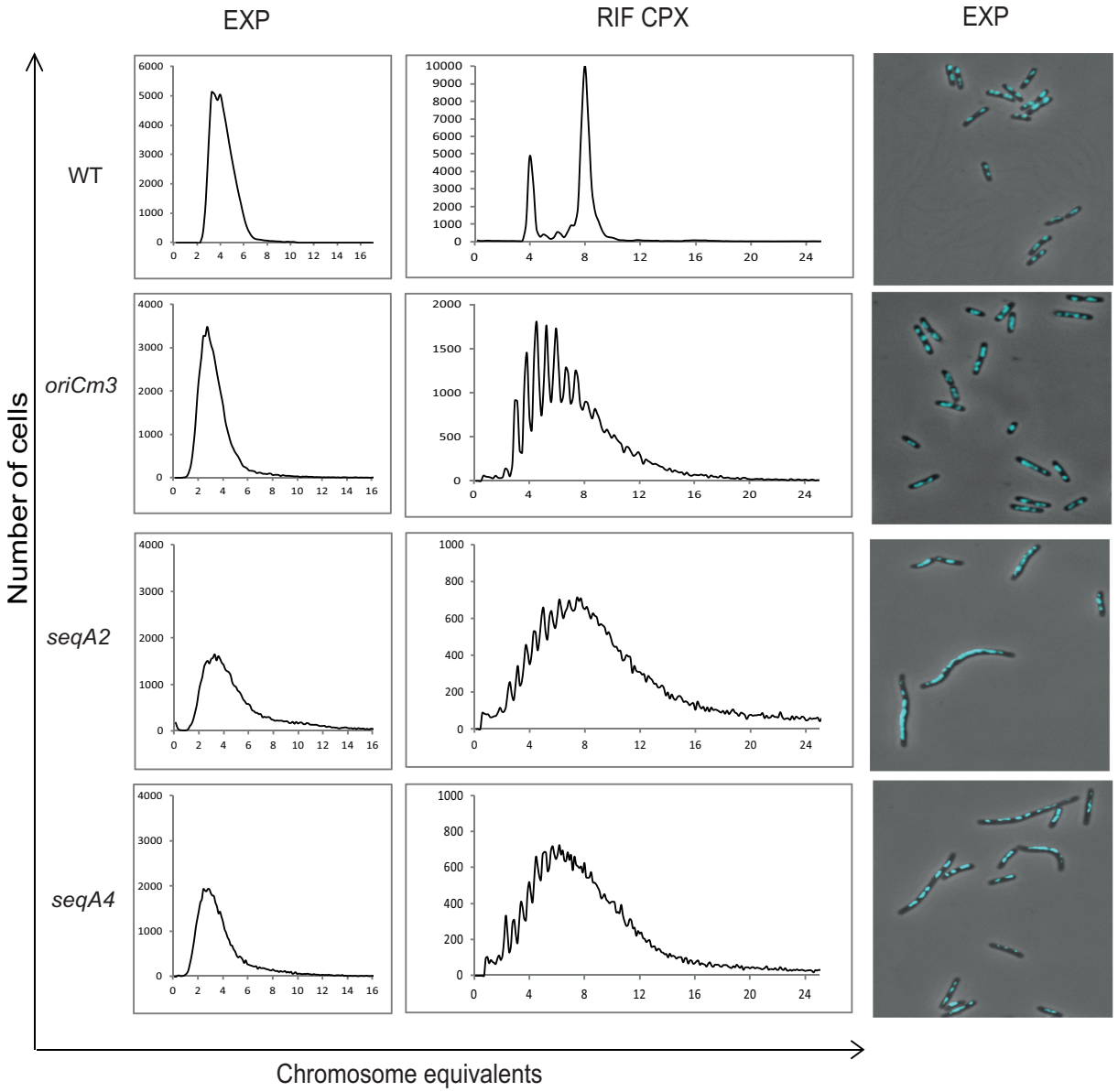


**Figure 3.** Lack of replication fork elongation and induction of the SOS response in the mutant *seqA2* and *seqA4* cells. Wild-type cells (MG1655), *oriCm3* mutant cells (IBP36), *seqA2* (IBP37) and *seqA4* (IBP38) mutant cells were grown in glucose–CAA at 37°C and analyzed by flow cytometry and microscopy. DNA histograms of exponentially growing cells (left panel) and run-out histograms of cells treated with rifampicin and cephalexin (see Materials and Methods) (middle panel) are shown. The chromosome equivalents (DNA content per cell) are shown on the abscissa and the number of cells per channel on the ordinate. Exponentially growing cells, fixed and stained with Hoechst, were also analyzed with phase contrast and fluorescence microscopy (see Materials and Methods) (right panel).

**Table 2.** Mean doubling time, mean relative cellular DNA content, mean relative mass and DNA/mass of the *seqA* mutants and the *oriCm3* mutant

| Strain | DT (min) ± STD | Relative DNA content ± STD | Relative mass ± STD | DNA/mass ± STD |
|---|---|---|---|---|
| Wild type (MG1655) | 25 ± 0.0 | 1.0 ± 0.0 | 1.0 ± 0.0 | 1.0 ± 0.0 |
| *oriCm3* (IBP36) | 25 ± 1.8 | 1.26 ± 0.1 | 1.14 ± 0.1 | 1.11 ± 0.0 |
| *seqA2* (IBP37) | 30 ± 0.6 | 1.96 ± 0.4 | 1.72 ± 0.5 | 1.19 ± 0.3 |
| *seqA4* (IBP38) | 29 ± 1 | 1.78 ± 0.3 | 1.43 ± 0.2 | 1.25 ± 0.1 |

in these mutants. The *seqA2*, *seqA4* and *oriCm3* mutations were transferred to a *recBC* temperature-sensitive strain, allowing us to inactivate RecBCD (53). These mutants exhibit no nuclease or recombination activity at the non-permissive temperature, so the amount of chromosomal fragmentation can be measured with PFGE. The Δ*seqA recBC*(Ts) double mutant was included as a positive control because it exhibits chromosomal fragmentation (40).

The *seqA* mutants of the temperature-sensitive strain had a significantly higher degree of chromosomal fragmentation compared to the *oriCm3* mutant (Figure 4; Supplementary Table S1). This result confirms that the *seqA* mutant cells experienced more problems during replication elongation than cells lacking only sequestration (*oriCm3*) and that the replication forks in *seqA* mutant cells disintegrate.

### The *seqA* mutants undergo direct DSBs

The above result showed that the *seqA2* and *seqA4* mutants exhibit chromosomal fragmentation when *recBC* is inactivated. Such large genomic fragments may arise from various abnormalities in replication fork elongation. PFGE of the *seqA2* and *seqA*4 single mutants did not reveal any significant fragmentation (i.e. without the *recBC* Ts mutation) (Supplementary Figure S1); thus, the chromosomal fragmentation in the *seqA* mutants is mostly repairable when RecBCD is active, as reported for the Δ*seqA* cells (40). However, chromosomal fragmentation in the absence of RecBCD could result from cleavage of reversed forks, as shown in Figure 1C, i. According to the RFR model, in the absence of RecBCD, the HJ is cleaved by RuvABC, and fragmentation can be observed by PFGE. This restart mechanism thus generates DSEs only when RecBCD is absent and is dependent on RuvABC. We were unable to construct *seqA2 or seqA4* strains lacking RuvAB (three rounds of unsuccessful transduction where controls were successful using the same lysate), however, possibly indicating that the *seqA* mutants depend on homologous recombination to survive.

To check whether this is the case, we also investigated their dependence on RecA. When we combined the two *seqA* mutations with a *recA* deletion, the viability of the *seqA2* and *seqA4* mutants decreased significantly (Figure 5A). This decrease was especially prominent when the *seqA recA* mutants were grown on LB agar, probably because of greater numbers of replication forks compared to growth on glucose–CAA agar (and the consequently higher demand for SeqA protein). The *seqA2* mutant also was somewhat less robust on LB agar than the *seqA4* mutant, as previously indicated from microscopy images and flow cytometry mass data (Figure 3; Table 2). Thus, *seqA* cells depend more than normal on homologous recombination, and DNA fragmentation results from formation of DSEs that require recombinational repair. The Δ*recA seqA2/4* co-inhibition is in accordance with results previously reported for Δ*seqA* strains (38,40). In contrast, *oriCm3* cells did not exhibit decreased viability when *recA* was deleted (Figure 5A), indicating that direct DSBs in the *seqA* mutants are attributable to an absence of functional SeqA in the cells rather than to over-replication because of a lack of sequestration.

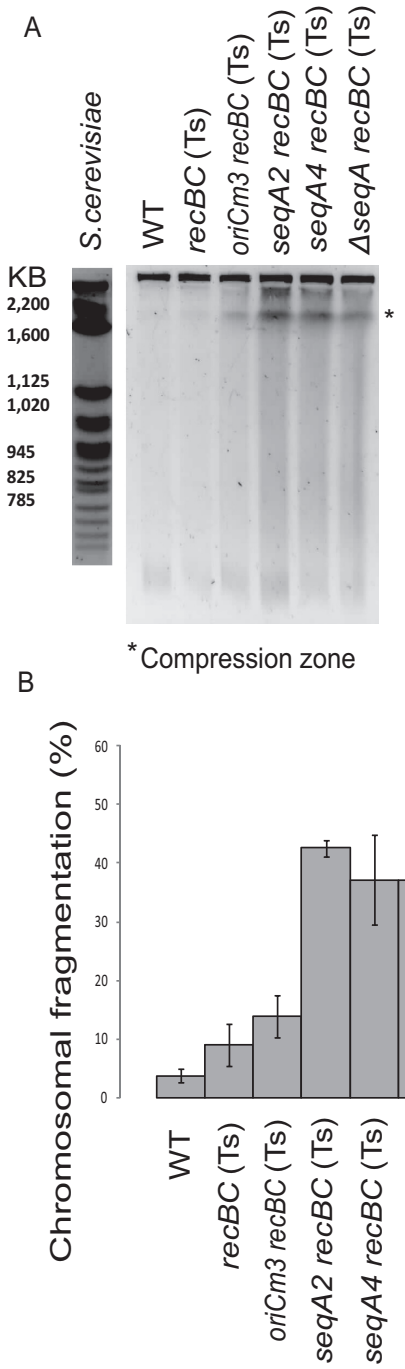


**Figure 4.** The *seqA2* and *seqA4* mutants exhibit significantly more chromosomal fragmentation compared to the *oriCm3* mutant. (**A**) Pulsed field gel electrophoresis of wild-type (AB1157), *recBC* (Ts) (SK129), *oriCm3 recBC* (Ts) (IBP04), *seqA2 recBC* (Ts) (IBP01), *seqA4 recBC* (Ts) (IBP03), and Δ*seqA recBC* (Ts) (ER89) after growth at 42°C in LB medium. Standard DNA from *S. cerevisiae* is shown to the left. The compression zone (containing large chromosomal fragments that are unable to move any further) is indicated with * (see Materials and Methods for more information). (**B**) Quantification of the chromosomal fragmentation found in (A). The amount of chromosomal fragmentation (%) was calculated by dividing the signal in the whole lane (excluding the well and the area right below the well) by the total signal (see Materials and Methods for more information). Error bars represent standard deviations.

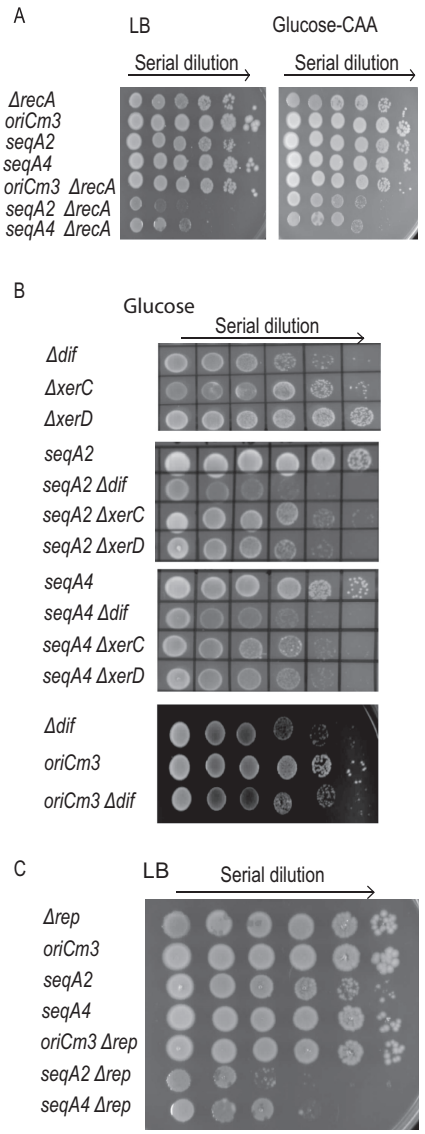


**Figure 5.** Loss of viability in the *seqA* mutants when combined with *ΔrecA*, *Δdif*, *ΔxerC*, *ΔxerD* or *Δrep*. Viability tests: Overnight cultures grown at 37°C were serially diluted and spotted on plates with the indicated medium. The spots are from left to right: undiluted and diluted $10^{-2}$, $10^{-3}$, $10^{-4}$, $10^{-5}$ and $10^{-6}$. (**A**) Viability tests of the *seqA2* Δ*recA* (IBP80), *seqA4* Δ*recA* (IBP81), and *oriCm3* Δ*recA* (IBP100) mutants, as well as the single mutants. (**B**) Viability tests of the *seqA2* Δ*dif* (IBP85), *seqA4* Δ*dif* (IBP82), *oriCm3* Δ*dif* (IBP101), *seqA2* Δ*xerC* (IBP74), *seqA4* Δ*xerC* (IBP83), *seqA2* Δ*xerD* (IBP68) and *seqA4* Δ*xerD* (IBP84) mutants, as well as the single mutants. (**C**) Viability tests of *seqA2* Δ*rep* (IBP40), *seqA4* Δ*rep* (IBP41) and *oriCm3* Δ*rep* (IBP98), as well as the single mutants.

## Dimer resolution is important for *seqA2* and *seqA4* mutant viability

Recombination and resolution of HJ may result in crossing over, leading to dimeric chromosomes (54–56). Resolution of a dimeric chromosome occurs at the *dif* site and is coupled to cell division (57). The multifunctional protein FtsK positions the *dif* sites to the septum and activates the tyrosine recombinases XerC and XerD, which in turn cut and rejoin the DNA, resolving the dimeric chromosome (reviewed in (57)). Because the *seqA* mutants seemed to depend on homologous recombination, we evaluated the effect of removing the *dif* site, XerC or XerD in these mutants. The cells grew poorly on rich media, so we conducted the viability test using glucose agar (to avoid suppressors). When only *dif*, XerC or XerD was removed, the mutants exhibited somewhat reduced viability, as demonstrated previously (58), indicating chromosomal dimers arise at a certain (low) frequency in otherwise normal cells (Figure 5B, top panel). However, in the double mutants, the viability was decreased compared to the single *dif*/*XerC*/*XerD* mutants (Figure 5B, middle panels). The effect was more prominent in *seqA2*/*4 dif* mutants compared to the *seqA2*/*4 xerC*/*xerD* mutants, presumably because cells may retain some dimer resolution activity when only XerC or XerD is deleted whereas all activity is lost in the *dif* cells in which XerCD cannot bind to the DNA. In summary, the results indicate a higher frequency of chromosomal dimers in *seqA* mutant cells compared to wild-type cells and elevated homologous recombinational activity. Removal of *dif* affected viability of *oriCm3* cells to the same extent as wild-type cells (Figure 5B, bottom panel), confirming that lack of sequestration alone does not lead to increased recombinational repair.

## The *seqA* mutants exhibit more 'reckless' degradation during replication run-out than the *oriCm3* mutant

To gather more information about the nature of replication fork rescue and restart in the *seqA* mutants, we investigated the so-called 'reckless' degradation caused by RecBCD in the absence of the RecA protein. *recA* (Ts) cells exhibit loss of entire chromosomes during replication fork run-out after treatment with rifampicin and cephalexin at the non-permissive temperature (59). A Δ*rep* mutant that also has elongation problems was included in the experiment for comparison (14,60–63). The Rep helicase helps clear obstacles at the replication fork (64) and interacts with the replicative helicase DnaB (65). Cells lacking Rep stall more frequently than normal and can restart the stalled forks through the RecBCD- and RuvABC-dependent remodeling reaction, which involves RFR and is independent of RecA (14). The *recA* (Ts) allele was combined with *oriCm3*, Δ*rep*, and *seqA* mutations and the resulting strains compared with the *recA* (Ts) single mutant by flow cytometry (see Table 3 for doubling times, DNA content, mass and DNA/mass values).

The loss of DNA during replication run-out in the absence of RecA function in the control cells (*recA* (Ts) at non-permissive compared to permissive temperatures was ∼15% (Figure 6A; Table 4), as can be seen in the run-out histogram (fewer cells in the four-chromosome peak, more cells in the three-chromosome peak; compare Figure 6B, *recA* (Ts) right panel and middle panel). It is not clear exactly which DNA is degraded during the replication run-out, but the most straightforward interpretation is that the DSE of a collapsed replication fork is bound by RecBCD and that this enzyme complex then degrades the entire 'daughter arm' of a partially replicated chromosome (66–68) (Figure 6C). Because RecA is non-functional, the degradation reaction will keep going past Chi sites and past *oriC* until the entire daughter arm is degraded and both replication forks elimi-

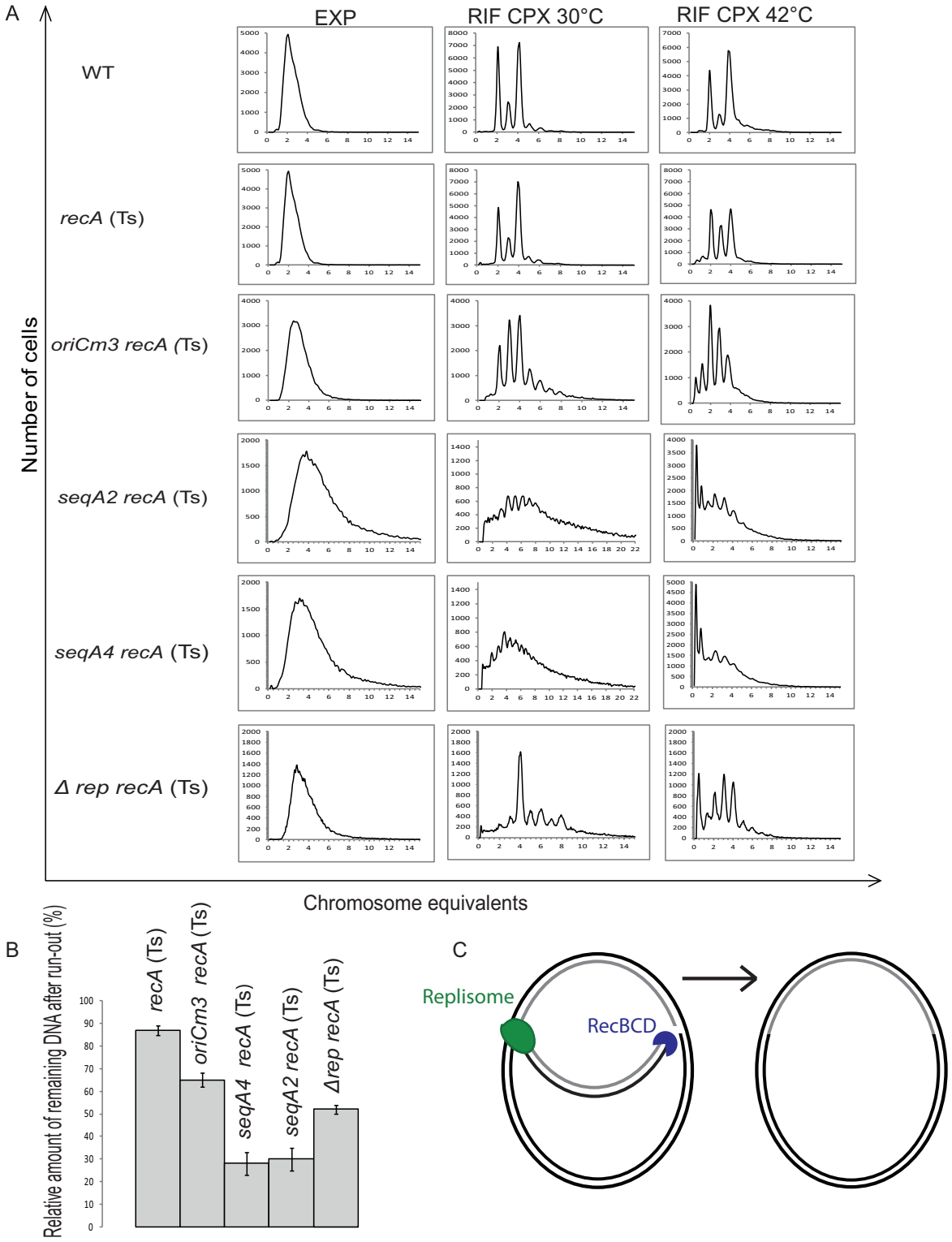


**Figure 6.** Degradation of DNA during run-out in the absence of RecA is extensive and does not yield integer numbers of chromosomes in the *seqA* mutants. (**A**) DNA histograms obtained by flow cytometry of wt (N1331), *recA* (Ts) (N1332), *oriCm3 recA* (Ts) (IBP07), *seqA2 recA* (Ts) (IBP02), *seqA4 recA* (Ts) (IBP06), and *Δrep recA* (Ts) (IBP24) grown in glucose–CAA medium. DNA histograms of cells growing exponentially at the permissive temperature (left panel), and run-out histograms of cells treated with rifampicin and cephalexin at the permissive (middle panel) and non-permissive (right panel) temperature are shown. (**B**) Bar plot showing the decrease in average number of chromosomes per cell during replication run-out in the absence of RecA function. Error bars represent standard deviations. (**C**) Model showing how DNA degradation by RecBCD in the absence of RecA may occur. In the model, collapse of the rightmost replication fork is shown. RecBCD binds to the resulting DSE and degrades the entire chromosome arm, eliminating both replication forks. The nicks are ligated, yielding one intact chromosome in a cell that under RecA+ conditions would have ended up with two chromosomes after replication run-out. The figure is adapted from (89).

**Table 3.** Mean doubling times, mean relative cellular DNA content, mean relative mass and DNA/mass of the *recA* (Ts) strains

| Strain | DT (min) ±STD | Relative DNA content ±STD | Relative mass ± STD | DNA/mass ± STD |
|---|---|---|---|---|
| Wild type (N1331) | 66 ± 4.0 | 1.0 ± 0.0 | 1.0 ± 0.0 | 1.0 ± 0.0 |
| *recA* (Ts) (N1332) | 69 ± 0.2 | 1.0 ± 0.0 | 1.1 ± 0.1 | 1.0 ± 0.0 |
| *oriCm3 recA* (Ts) (IBP07) | 70 ± 0.6 | 1.3 ± 0.1 | 1.5 ± 0.1 | 0.9 ± 0.0 |
| *seqA2 recA* (Ts) (IBP02) | 85 ± 3.0 | 2.4 ± 0.3 | 2.4 ± 0.4 | 1.0 ± 0.1 |
| *seqA4 recA* (Ts) (IBP06) | 87 ± 2.7 | 2.2 ± 0.2 | 2.2 ± 0.1 | 1.0 ± 0.1 |
| Δ*rep recA* (Ts) (IBP24) | 73 ± 1.0 | 1.61 ± 0.0 | 2.07 ± 0.2 | 0.79 ± 0.1 |

nated (Figure 6C). The *recA* (Ts) control cells have a replication pattern in which initiation occurs at two origins and the cells have two replicating chromosomes with two forks each. If one of the forks encounters an obstacle or nick that causes the fork to collapse and a daughter arm to be degraded, after replication run-out, the cell will contain three chromosomes instead of four.

The amount of degradation in the *oriCm3 recA*(Ts) mutant was ∼35% (Figure 6A; Table 4), and as in the *recA*(Ts) mutant, most of the cellular DNA was found as integer numbers of chromosomes (Figure 6B). The reason for the increased amount of degradation may be that an increased number of forks and more closely spaced forks (caused by asynchrony and over-initiation) led to an increase number of collapsed forks. Likewise, in the Δ*rep recA*(Ts) cells, integer numbers of chromosomes dominated, indicating that in the absence of RecA, collapsed fork arms were fully degraded but that much of the chromosomal DNA stayed intact (Figure 6B). The increased amount of fork stalling in the absence of Rep protein led to ∼45% degradation during RecA-less replication run-out (Figure 6A; Table 4).

The *seqA recA*(Ts) mutants, on the other hand, showed a lack of histogram peaks after RecA-less replication run-out (Figure 6B) and also extensive degradation (∼70%) (Figure 6A; Table 4). The greater degradation in the *seqA recA*(Ts) mutants compared to the *oriCm3 recA*(Ts) mutant and the Δ*rep recA*(Ts) mutant indicates that DSEs occurred more frequently in the *seqA recA*(Ts) mutants, possibly because Δ*rep* cells restart stalled or paused replication forks directly (without homologous recombination) by the RecBCD-dependent modulation of the stalled fork (see Figure 1C, iii) (14). Thus, in Δ*rep* cells, collapse of forks would lead to degradation during RecA-less replication run-out. The results indicate that in the absence of SeqA function, more forks collapse directly, more rear-ending of forks occurs, or both events take place. The results are in accordance with the absence of peaks in histograms of *seqA2* and *seqA4* cultures after growth in run-out conditions in the presence of RecA (Figure 6B, middle panels; Figure 3).

### Replication fork remodeling may not be possible in *seqA* mutants

Stabilization of DNA (200–300 nm) between the SeqA structure and the replisome (37) might be beneficial for replication fork re-start after replication fork stalling or disintegration. Loss of this stabilized area (i.e. by lack of SeqA) thus could affect such replication fork reactions. To investigate a scenario in which replication forks pause and stall more frequently than normal, we combined the *seqA* and *oriCm3* mutations with *Δrep.* As noted, when Rep helicase is missing, replication forks stall more frequently and can be restarted by a remodeling reaction probably involving RFR (14). If the remodeling reaction requires SeqA, the double mutants would be expected to show a loss of viability.

In accordance with previous findings (61), the Δ*rep* single mutant cells showed the expected run-out histogram with clear peaks (Figure 6A, bottom row, middle column), indicating that the replication forks could complete replication. Thus, although replication forks stalled more frequently in *rep*-deleted cells, they seem to be restarted rather efficiently through direct restart mechanisms (see Figure 1C, iii) and still reached *ter* without a significantly affected doubling time (Table 3).

In contrast, cells with either *seqA2* or *seqA4* in combination with *rep* deletion displayed a significantly decreased viability compared to single mutants (Figure 5C), as has been shown for *ΔseqA rep* cells (69). However, the combination of *oriCm3* with the *rep* deletion did not produce this result, possibly indicating that replication forks stalled because of absent Rep helicase are not managed the same way without SeqA as they are with SeqA (i.e. by direct restart mechanisms, at least some of which involve RFR) (see Figure 1C, iii). The unchanged viability of the *oriCm3* Δ*rep* cells shows that an increased number of replication forks is not the sole factor leading to greater difficulty for Δ*rep* cells also carrying mutations in *seqA.*

### Microscopy and flow cytometry of Gam-GFP indicates occurrence of DSEs in the *seqA* mutants

For further evidence of the occurrence of DSEs in *seqA* mutants, we used a *Gam-GFP* construct controlled by a doxycycline/tetracycline-inducible promoter (kindly provided by S. Rosenberg (70)). The Gam protein originates from the Mu phage and binds and protects DSEs of linear DNA, thus inhibiting exonuclease activity (71) and subsequently recombinational repair (70). Gam-GFP can therefore be used to visualize DSEs in living cells because it forms fluorescent foci upon DNA DSE binding.

The *seqA* mutants containing the *gam-GFP* construct were investigated using fluorescence microscopy and flow cytometry, together with the wild-type equivalent (MG1655 *gam-GFP*). When visualized with fluorescence microscopy, both the wild-type and the *seqA* mutants showed a weak background of Gam-GFP fluorescence (pseudo-colored blue, Figure 7A). However, in contrast to the wild-type cells, many of the *seqA* mutant cells contained structures with a strong GFP signal, and a few cells contained distinct foci (pseudo-colored magenta, Figure 7A).

To quantify the number of cells containing high-intensity Gam-GFP signal, we analyzed 50 000 cells per sample us-

**Table 4.** Mean number of chromosomes/cell after replication run-out and decrease representing reckless degradation after inactivation of RecA

| Strain | Chromosomes/cell 30°C ± STD | Chromosomes/cell 42°C ± STD | % Change ± STD |
|---|---|---|---|
| Wild type (N1331) | 3.4 ± 0.1 | 3.5 ± 0.1 | |
| *recA* (Ts) (N1332) | 3.5 ± 0.0 | 3.0 ± 0.1 | 13 ± 2.4 |
| *oriCm3 recA* (Ts) (IBP07) | 4.3 ± 0.1 | 2.8 ± 0.1 | 35 ± 3.1 |
| *seqA2 recA* (Ts) (IBP02) | 8.5 ± 0.1 | 2.4 ± 0.4 | 72 ± 4.9 |
| *seqA4 recA* (Ts) (IBP06) | 7.8 ± 0.5 | 2.3 ± 0.3 | 70 ± 5.4 |
| Δ*rep recA* (Ts) (IBP24) | 5.6 ± 0.2 | 2.7 ± 0.2 | 46 ± 3.6 |

ing flow cytometry. Shee *et al.* (70) reported that ∼7.5% of wild-type cells contained Gam-GFP foci as a result of spontaneous DSBs, so we gated the scatter plot of the wild-type cells (GFP signal versus cell size/forward scatter) according to this value. Because background Gam-GFP fluorescence could be observed in all cells, only cells with greater-than-expected GFP intensity based on cell size were included. The gating threshold for defining high- and low-intensity values (respective to cell size) was copied to the scatter plots of the *seqA* mutant cells. The fraction of the population containing GFP signal above the set intensity threshold yielded, on average, 16.2% and 15.9% for the *seqA2* and *seqA4* mutant cells, respectively (Figure 7B). The implication is that more than twice as many cells contained DSEs in the *seqA* mutant populations compared to the wild-type population.

These results support our previous inferences that DSEs are generated during replication in the *seqA* mutants and that rear-ending of forks, a lack of direct restart of forks, or both may occur in the absence of SeqA function.

## DISCUSSION

### Lack of SeqA complexes behind the replication forks leads to replication fork disintegration

We show in this work that both *seqA2* and *seqA4* mutant cells display signs of disintegrated replication forks, resulting in formation of DSEs and rendering these cells dependent on homologous recombination. The observed phenotypes of cells lacking SeqA function are in accordance with previous microarray studies showing that cells without SeqA have an increased *oriC*/*ter* ratio and aberrant frequency of gene markers between the origin and the terminus when growing exponentially (40,69). In those studies, the frequency of genes did not follow an exponential pattern but increased in the origin-proximal half of the chromosome, which indicates that not all replication forks launched at *oriC* reach the terminus within a reasonable amount of time. Both these earlier results and our current findings thus indicate that replication forks disintegrate in cells without proper SeqA function. In contrast, *oriCm3* cells performed replication run-out and were not abnormally dependent on recombination enzymes. Together, these findings indicate that (i) binding of fully functional SeqA behind the replication fork can protect cells against formation of DSEs during replication and (ii) the chromosomal fragmentation observed in the *seqA* mutants is not merely a result of an increased number of replication forks.

Rotman *et al.* (40) proposed that segregation of sister chromosomes could be the source of DSEs in the absence of SeqA behind the replication forks. In this model, the lack of the SeqA barrier would cause the 'segregation fork' to collide with a stalled replication fork, leading to a rupture at a single-stranded region as the segregation machinery pulls the sister strands apart. Although SeqA has been proposed to delay separation of newly synthesized DNA (72), the segregation fork model is not concordant with studies of loci segregation after replication or with differences in SeqA requirements during slow and rapid growth. Loss of SeqA affects the growth rate of rapidly growing but not slowly growing cells (73), indicating that its functions are more important during rapid growth. However, in rapidly growing cells, the replication period spans several generations, so that newly replicated sister molecules reside in the same cell half and co-segregate (36,37) (Figure 8A). Thus, the increased demand for SeqA during rapid growth does not fit with the 'segregation fork' hypothesis because the two sister DNA molecules behind a fork do not segregate before cell division during rapid growth. Moreover, in slowly growing cells in which the 'segregation fork' in theory could pose a threat to the replication fork (because the sister DNA molecules are segregated to each cell half; Figure 8B), replicated loci stay co-localized for 10–20 min (74). We therefore find it more likely that the observed chromosomal fragmentation in the *seqA* mutants arises from challenges during chromosome replication rather than from segregation issues.

### The dynamic SeqA structures trailing the replication forks might prevent rear-ending

A DSE can theoretically arise if a replication fork catches up with an 'older' replication fork in front and replicates the last nucleotide of the newly synthesized strand, the so-called rear-ending (75–78) (Figure 1A, ii). Replication forks stall from time to time (7,61), so replication forks could possibly catch up with each other, especially if sequestration (which causes spacing between the forks of about one third of a generation) is absent. SeqA complexes bound to hemi-methylated DNA trailing the replication fork might delay progression of replication forks approaching from behind, helping to prevent rear-ending collisions (Figure 2B). The rear-ending model thus offers a possible explanation for the formation of DSEs in the *seqA* mutants, which both over-initiate and lack the proper SeqA complexes behind the fork.

A recent study found that rear-ending does not seem to be the source of DSEs when SeqA is absent (40); however, whether the applied method had sufficient sensitivity to exclude this possibility is uncertain. We show here that DSEs are generated during replication run-out in cells lacking SeqA, a problem that increases with the number of forks following each other on a chromosome. Thus, we argue that it

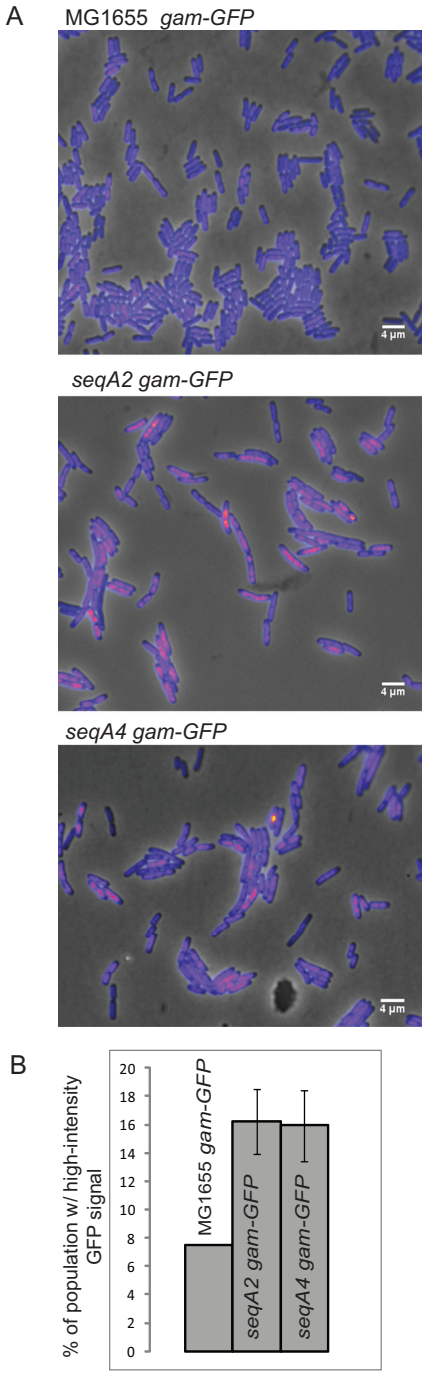


**Figure 7.** Analysis of Gam-GFP signal using fluorescence microscopy and flow cytometry indicates that DSEs arise in the *seqA* mutants. (**A**) Fluorescence microscopy of Gam-GFP in wild-type (EH137), *seqA2* (EH138) and *seqA4* (EH139) mutant cells grown in glucose–CAA at 37°C after 1 h of induction with anhydrotetracycline (10 ng/ml). The GFP-signal is pseudo-colored according to pixel intensity, in which blue represents weak background signal and magenta represents higher intensity values. (**B**) Bar plot showing the percentage of the cell population containing high-intensity Gam-GFP signal deduced from flow cytometry analysis of GFP in 50 000 cells for wild-type (EH137), *seqA2* (EH138) and *seqA4* (EH139) mutant strains after 1 h of induction with anhydrotetracycline (10 ng/ml). The gating threshold for definition of high- and low-intensity values was set according to the reported fraction of wild-type cells containing Gam-GFP foci due to spontaneous DSBs (7.5%) (70). Error bars represent standard error of the mean (SEM).

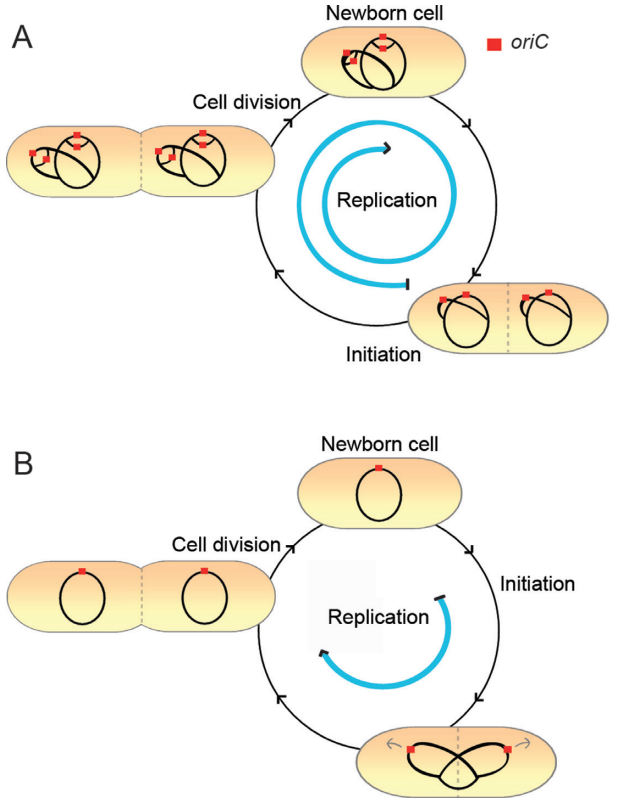


**Figure 8.** Newly replicated sister DNA molecules are segregated to each cell half during slow growth but not during rapid growth. (**A**) Schematic and simplified figure of the replication pattern and chromosome localization for MG1655 cells grown in glucose-CAA medium at 37°C. The sister DNA from each chromosome co-segregates to each cell half. (**B**) Schematic and simplified figure of the replication pattern and chromosome localization for MG1655 cells grown in minimal medium at 37°C. The cells contain only one replicating chromosome, and the sister DNA is thus segregated to each cell half.

is highly likely that some of the DSEs present in cells lacking SeqA trace to rear-ending of replication forks. This inference seem reasonable because the SeqA protein can prevent rear-ending in two ways: by sequestration, which provides a minimum space between forks (rounds of replication), and by forming a protein barrier that may delay the progress of a new fork moving toward the old one.

### Binding of SeqA behind the replication fork might facilitate restart of stalled replication forks

Rear-ending may not be the only problem in cells lacking SeqA function, however. Massive over-initiation because of unregulated levels of ATP-DnaA is reported to lead to cell death as replisomes run into nicks arising from partial oxidative damage repair (79), forming DSEs that apparently exhaust the homologous recombination repair capacity. Cells lacking SeqA function do not over-initiate to this extent, but slow repair of damage relative to the number of ongoing replication forks also could be a problem in the absence of SeqA. A third issue in cells lacking SeqA function could be that 'easy' or 'direct' restart of stalled replication forks, i.e. restart that does not require homologous recombination, functions poorly. The stretch of DNA be-

tween the SeqA complexes trailing the fork and the replisome may be an optimal location for replication fork repair and restart reactions. For instance, replication fork remodeling processes such as RFR may be more easily accommodated, as suggested in the model shown in Figure 2A. The reduced viability of the Δ*rep seqA* mutants could point toward a deficiency in restart. Replication forks in Δ*rep* cells frequently stall and restart via direct restart mechanisms (14). The *oriCm3* cells over-initiate in the same manner as the *seqA* mutants (i.e., because of lack of sequestration) but can exhibit frequent replication restart in the absence of Rep protein (successful elongation of replication by flow cytometry). Thus, an increased number of replication forks is not the reason for the loss of viability in combination with *seqA* mutation. The cells without Rep are especially dependent on direct restart of replication forks and on the presence of SeqA at the forks, so the result may indicate that the SeqA structures somehow facilitate replication fork restart mechanisms. Binding of SeqA at a distance behind the replisome might provide a stabilized area necessary for such replication fork restart reactions to occur (Figure 2A). It is also possible that SeqA actively participates in restart of stalled forks via a so far unknown reaction.

In summary, we find it likely that replication elongation problems in cells without SeqA function stem from a combination of replication fork rear-ending and deficiencies that occur from aberrant handling of the nascent strands, such as lack of direct replication fork restart.

## SUPPLEMENTARY DATA

Supplementary Data are available at NAR Online.

## ACKNOWLEDGEMENTS

We thank Frank Sætre and Anne Wahl for excellent technical assistance and Knut Ivan Kristiansen and James Booth for critical reading of the manuscript. We are grateful to the Department of Radiation Biology, The Norwegian Radium Hospital, for sharing their flow cytometry facility, and to Trond Stokke, Kirsti Solberg Landsverk, and Idun Dale Rein for technical assistance with the LSR II. We thank A. Kuzminov, D. Sherratt and S. Rosenberg for providing strains.

## FUNDING

Norwegian Research Council [197102]; Helse Sør-Øst [2011028]. Funding for open access charge: Helse Sør-Øst.
*Conflict of interest statement.* None declared.

## REFERENCES

1. Kornberg,A. and Baker,T.A. (1992) *DNA Replication*. W.H. Freeman and Company, NY.
2. Yeeles,J.T., Poli,J., Marians,K.J. and Pasero,P. (2013) Rescuing stalled or damaged replication forks. *Cold Spring Harbor Perspect. Biol.*, **5**, a012815.
3. Kogoma,T. (1997) Stable DNA replication: interplay between DNA replication, homologous recombination, and transcription. *Microbiol. Mol. Biol. Rev.: MMBR*, **61**, 212–238.
4. Kreuzer,K.N. (2005) Interplay between DNA replication and recombination in prokaryotes. *Annu. Rev. Microbiol.*, **59**, 43–67.
5. Michel,B., Boubakri,H., Baharoglu,Z., LeMasson,M. and Lestini,R. (2007) Recombination proteins and rescue of arrested replication forks. *DNA Repair*, **6**, 967–980.
6. Michel,B., Grompone,G., Flores,M.J. and Bidnenko,V. (2004) Multiple pathways process stalled replication forks. *Proc. Natl. Acad. Sci. U.S.A.*, **101**, 12783–12788.
7. Mettrick,K.A. and Grainge,I. (2016) Stability of blocked replication forks *in vivo*. *Nucleic Acids Res.*, **44**, 657–668.
8. Cox,M.M., Goodman,M.F., Kreuzer,K.N., Sherratt,D.J., Sandler,S.J. and Marians,K.J. (2000) The importance of repairing stalled replication forks. *Nature*, **404**, 37–41.
9. Kuzminov,A. (1995) Instability of inhibited replication forks in *E. coli*. *BioEssays*, **17**, 733–741.
10. Lusetti,S.L. and Cox,M.M. (2002) The bacterial RecA protein and the recombinational DNA repair of stalled replication forks. *Annu. Rev. Biochem.*, **71**, 71–100.
11. Michel,B. and Leach,D. (2012) Homologous recombination—enzymes and pathways. *EcoSal Plus*, **5**, doi:10.1128/ecosalplus.7.2.7.
12. Sandler,S.J. and Marians,K.J. (2000) Role of PriA in replication fork reactivation in *Escherichia coli*. *J. Bacteriol.*, **182**, 9–13.
13. Yeeles,J.T. and Marians,K.J. (2013) Dynamics of leading-strand lesion skipping by the replisome. *Mol. Cell*, **52**, 855–865.
14. Seigneur,M., Bidnenko,V., Ehrlich,S.D. and Michel,B. (1998) RuvAB acts at arrested replication forks. *Cell*, **95**, 419–430.
15. Seigneur,M., Ehrlich,S.D. and Michel,B. (2000) RuvABC-dependent double-strand breaks in dnaBts mutants require recA. *Mol. Microbiol.*, **38**, 565–574.
16. McGlynn,P., Lloyd,R.G. and Marians,K.J. (2001) Formation of Holliday junctions by regression of nascent DNA in intermediates containing stalled replication forks: RecG stimulates regression even when the DNA is negatively supercoiled. *Proc. Natl. Acad. Sci. U.S.A.*, **98**, 8235–8240.
17. Campbell,J.L. and Kleckner,N. (1990) *E. coli oriC* and the *dnaA* gene promoter are sequestered from dam methyltransferase following the passage of the chromosomal replication fork. *Cell*, **62**, 967–979.
18. Lu,M., Campbell,J.L., Boye,E. and Kleckner,N. (1994) SeqA: a negative modulator of replication initiation in *E. coli*. *Cell*, **77**, 413–426.
19. Russell,D.W. and Zinder,N.D. (1987) Hemimethylation prevents DNA replication in *E. coli*. *Cell*, **50**, 1071–1079.
20. von Freiesleben,U., Rasmussen,K.V. and Schaechter,M. (1994) SeqA limits DnaA activity in replication from *oriC* in *Escherichia coli*. *Mol. Microbiol.*, **14**, 763–772.
21. Skarstad,K., Boye,E. and Steen,H.B. (1986) Timing of initiation of chromosome replication in individual *Escherichia coli* cells. *EMBO J.*, **5**, 1711–1717.
22. Skarstad,K. and Lobner-Olesen,A. (2003) Stable co-existence of separate replicons in *Escherichia coli* is dependent on once-per-cell-cycle initiation. *EMBO J.*, **22**, 140–150.
23. Waldminghaus,T. and Skarstad,K. (2009) The *Escherichia coli* SeqA protein. *Plasmid*, **61**, 141–150.
24. Sánchez-Romero,M.A., Busby,S.J., Dyer,N.P., Ott,S., Millard,A.D. and Grainger,D.C. (2010) Dynamic distribution of SeqA protein across the chromosome of *Escherichia coli* K-12. *MBio*, **1**, doi:10.1128/mBio.00012-10.
25. Bach,T. and Skarstad,K. (2005) An *oriC*-like distribution of GATC sites mediates full sequestration of non-origin sequences in *Escherichia coli*. *J. Mol. Biol.*, **350**, 7–11.
26. Slater,S., Wold,S., Lu,M., Boye,E., Skarstad,K. and Kleckner,N. (1995) *E. coli* SeqA protein binds *oriC* in two different methyl-modulated reactions appropriate to its roles in DNA replication initiation and origin sequestration. *Cell*, **82**, 927–936.
27. Waldminghaus,T., Weigel,C. and Skarstad,K. (2012) Replication fork movement and methylation govern SeqA binding to the *Escherichia coli* chromosome. *Nucleic Acids Res.*, **40**, 5465–5476.
28. von Freiesleben,U., Krekling,M.A., Hansen,F.G. and Lobner-Olesen,A. (2000) The eclipse period of *Escherichia coli*. *EMBO J.*, **19**, 6240–6248.
29. Brendler,T., Sawitzke,J., Sergueev,K. and Austin,S. (2000) A case for sliding SeqA tracts at anchored replication forks during *Escherichia coli* chromosome replication and segregation. *EMBO J.*, **19**, 6249–6258.

30. Fossum,S., Crooke,E. and Skarstad,K. (2007) Organization of sister origins and replisomes during multifork DNA replication in *Escherichia coli*. *EMBO J.*, **26**, 4514–4522.
31. Hiraga,S., Ichinose,C., Niki,H. and Yamazoe,M. (1998) Cell cycle-dependent duplication and bidirectional migration of SeqA-associated DNA-protein complexes in *E. coli*. *Mol. Cell*, **1**, 381–387.
32. Molina,F. and Skarstad,K. (2004) Replication fork and SeqA focus distributions in *Escherichia coli* suggest a replication hyperstructure dependent on nucleotide metabolism. *Mol. Microbiol.*, **52**, 1597–1612.
33. Onogi,T., Niki,H., Yamazoe,M. and Hiraga,S. (1999) The assembly and migration of SeqA-Gfp fusion in living cells of *Escherichia coli*. *Mol. Microbiol.*, **31**, 1775–1782.
34. Yamazoe,M., Adachi,S., Kanaya,S., Ohsumi,K. and Hiraga,S. (2005) Sequential binding of SeqA protein to nascent DNA segments at replication forks in synchronized cultures of *Escherichia coli*. *Mol. Microbiol.*, **55**, 289–298.
35. Adachi,S., Fukushima,T. and Hiraga,S. (2008) Dynamic events of sister chromosomes in the cell cycle of *Escherichia coli*. *Genes Cells*, **13**, 181–197.
36. Fossum-Raunehaug,S., Helgesen,E., Stokke,C. and Skarstad,K. (2014) *Escherichia coli* SeqA structures relocalize abruptly upon termination of origin sequestration during multifork DNA replication. *PLoS One*, **9**, e110575.
37. Helgesen,E., Fossum-Raunehaug,S., Saetre,F., Schink,K.O. and Skarstad,K. (2015) Dynamic *Escherichia coli* SeqA complexes organize the newly replicated DNA at a considerable distance from the replisome. *Nucleic Acids Res.*, **43**, 2730–2743.
38. Kouzminova,E.A., Rotman,E., Macomber,L., Zhang,J. and Kuzminov,A. (2004) RecA-dependent mutants in *Escherichia coli* reveal strategies to avoid chromosomal fragmentation. *Proc. Natl. Acad. Sci. U.S.A.*, **101**, 16262–16267.
39. Rotman,E., Bratcher,P. and Kuzminov,A. (2009) Reduced lipopolysaccharide phosphorylation in *Escherichia coli* lowers the elevated ori/ter ratio in seqA mutants. *Mol. Microbiol.*, **72**, 1273–1292.
40. Rotman,E., Khan,S.R., Kouzminova,E. and Kuzminov,A. (2014) Replication fork inhibition in seqA mutants of *Escherichia coli* triggers replication fork breakage. *Mol. Microbiol.*, **93**, 50–64.
41. Fossum,S., Soreide,S. and Skarstad,K. (2003) Lack of SeqA focus formation, specific DNA binding and proper protein multimerization in the *Escherichia coli* sequestration mutant seqA2. *Mol. Microbiol.*, **47**, 619–632.
42. Odsbu,I., Klungsoyr,H.K., Fossum,S. and Skarstad,K. (2005) Specific N-terminal interactions of the *Escherichia coli* SeqA protein are required to form multimers that restrain negative supercoils and form foci. *Genes Cells*, **10**, 1039–1049.
43. Bach,T. and Skarstad,K. (2004) Re-replication from non-sequesterable origins generates three-nucleoid cells which divide asymmetrically. *Mol. Microbiol.*, **51**, 1589–1600.
44. Clark,D. and Maaløe,O. (1967) DNA replication and the division cycle in *Escherichia coli*. *J. Mol. Biol.*, **23**, 99–112.
45. Datsenko,K.A. and Wanner,B.L. (2000) One-step inactivation of chromosomal genes in *Escherichia coli* K-12 using PCR products. *Proc. Natl. Acad. Sci. U.S.A.*, **97**, 6640–6645.
46. Miller,J.H. (1992) *A Short Course in Bacterial Genetics*. Cold Spring Harbor Laboratory Press.
47. Hillier,A.J. and Davidson,B.E. (1995) Pulsed field gel electrophoresis. *Methods Mol. Biol. (Clifton, N.J.)*, **46**, 149–164.
48. Gradzka,I. and Iwanenko,T. (2005) A non-radioactive, PFGE-based assay for low levels of DNA double-strand breaks in mammalian cells. *DNA Repair*, **4**, 1129–1139.
49. Repar,J., Briski,N., Buljubasic,M., Zahradka,K. and Zahradka,D. (2013) Exonuclease VII is involved in "reckless" DNA degradation in UV-irradiated *Escherichia coli*. *Mutat. Res.*, **750**, 96–104.
50. Wold,S., Skarstad,K., Steen,H.B., Stokke,T. and Boye,E. (1994) The initiation mass for DNA replication in *Escherichia coli* K-12 is dependent on growth rate. *EMBO J.*, **13**, 2097–2102.
51. Torheim,N.K., Boye,E., Lobner-Olesen,A., Stokke,T. and Skarstad,K. (2000) The *Escherichia coli* SeqA protein destabilizes mutant DnaA204 protein. *Mol. Microbiol.*, **37**, 629–638.
52. Odsbu,I. and Skarstad,K. (2014) DNA compaction in the early part of the SOS response is dependent on RecN and RecA. *Microbiology (Reading, England)*, **160**, 872–882.
53. Kushner,S.R. (1974) *In vivo* studies of temperature-sensitive *recB* and *recC* mutants. *J. Bacteriol.*, **120**, 1213–1218.
54. Friedberg,E.C., Walker,G.C., Siede,W., Wood,R.D., Schultz,R.A. and Ellenberger,T. (2006) *DNA Repair and Mutagenesis*. ASM press, Washington DC.
55. Kuzminov,A. (1999) Recombinational repair of DNA damage in *Escherichia coli* and bacteriophage lambda. *Microbiol. Mol. Biol. Rev.: MMBR*, **63**, 751–813.
56. Steiner,W.W. and Kuempel,P.L. (1998) Sister chromatid exchange frequencies in *Escherichia coli* analyzed by recombination at the *dif* resolvase site. *J. Bacteriol.*, **180**, 6269–6275.
57. Lesterlin,C., Barre,F.X. and Cornet,F. (2004) Genetic recombination and the cell cycle: what we have learned from chromosome dimers. *Mol. Microbiol.*, **54**, 1151–1160.
58. Ting,H., Kouzminova,E.A. and Kuzminov,A. (2008) Synthetic lethality with the dut defect in *Escherichia coli* reveals layers of DNA damage of increasing complexity due to uracil incorporation. *J. Bacteriol.*, **190**, 5841–5854.
59. Skarstad,K. and Boye,E. (1993) Degradation of individual chromosomes in recA mutants of *Escherichia coli*. *J. Bacteriol.*, **175**, 5505–5509.
60. Atkinson,J., Gupta,M.K., Rudolph,C.J., Bell,H., Lloyd,R.G. and McGlynn,P. (2011) Localization of an accessory helicase at the replisome is critical in sustaining efficient genome duplication. *Nucleic Acids Res.*, **39**, 949–957.
61. Gupta,M.K., Guy,C.P., Yeeles,J.T., Atkinson,J., Bell,H., Lloyd,R.G., Marians,K.J. and McGlynn,P. (2013) Protein-DNA complexes are the primary sources of replication fork pausing in *Escherichia coli*. *Proc. Natl. Acad. Sci. U.S.A.*, **110**, 7252–7257.
62. Guy,C.P., Atkinson,J., Gupta,M.K., Mahdi,A.A., Gwynn,E.J., Rudolph,C.J., Moon,P.B., van Knippenberg,I.C., Cadman,C.J., Dillingham,M.S. *et al.* (2009) Rep provides a second motor at the replisome to promote duplication of protein-bound DNA. *Mol. Cell*, **36**, 654–666.
63. Lane,H.E. and Denhardt,D.T. (1974) The rep mutation. III. Altered structure of the replicating *Escherichia coli* chromosome. *J. Bacteriol.*, **120**, 805–814.
64. Matson,S.W., Bean,D.W. and George,J.W. (1994) DNA helicases: enzymes with essential roles in all aspects of DNA metabolism. *BioEssays*, **16**, 13–22.
65. Bruning,J.G., Howard,J.L. and McGlynn,P. (2014) Accessory replicative helicases and the replication of protein-bound DNA. *J. Mol. Biol.*, **426**, 3917–3928.
66. Horiuchi,T. and Fujimura,Y. (1995) Recombinational rescue of the stalled DNA replication fork: a model based on analysis of an *Escherichia coli* strain with a chromosome region difficult to replicate. *J. Bacteriol.*, **177**, 783–791.
67. Kuzminov,A. and Stahl,F.W. (1997) Stability of linear DNA in *recA* mutant *Escherichia coli* cells reflects ongoing chromosomal DNA degradation. *J. Bacteriol.*, **179**, 880–888.
68. Uzest,M., Ehrlich,S.D. and Michel,B. (1995) Lethality of *rep recB* and *rep recC* double mutants of *Escherichia coli*. *Mol. Microbiol.*, **17**, 1177–1188.
69. Khan,S.R., Mahaseth,T., Kouzminova,E.A., Cronan,G.E. and Kuzminov,A. (2016) Static and dynamic factors limit chromosomal replication complexity in *Escherichia coli*, avoiding dangers of runaway overreplication. *Genetics*, **202**, 945–960.
70. Shee,C., Cox,B.D., Gu,F., Luengas,E.M., Joshi,M.C., Chiu,L.Y., Magnan,D., Halliday,J.A., Frisch,R.L., Gibson,J.L. *et al.* (2013) Engineered proteins detect spontaneous DNA breakage in human and bacterial cells. *eLife*, **2**, e01222.
71. Abraham,Z.H. and Symonds,N. (1990) Purification of overexpressed gam gene protein from bacteriophage Mu by denaturation-renaturation techniques and a study of its DNA-binding properties. *The Biochem. J.*, **269**, 679–684.
72. Joshi,M.C., Magnan,D., Montminy,T.P., Lies,M., Stepankiw,N. and Bates,D. (2013) Regulation of sister chromosome cohesion by the replication fork tracking protein SeqA. *PLoS Genet.*, **9**, e1003673.
73. Boye,E., Stokke,T., Kleckner,N. and Skarstad,K. (1996) Coordinating DNA replication initiation with cell growth: differential roles for DnaA and SeqA proteins. *Proc. Natl. Acad. Sci. U.S.A.*, **93**, 12206–12211.

74. Nielsen,H.J., Li,Y., Youngren,B., Hansen,F.G. and Austin,S. (2006) Progressive segregation of the *Escherichia coli* chromosome. *Mol. Microbiol.*, **61**, 383–393.
75. Bidnenko,V., Ehrlich,S.D. and Michel,B. (2002) Replication fork collapse at replication terminator sequences. *EMBO J.*, **21**, 3898–3907.
76. Grigorian,A.V., Lustig,R.B., Guzman,E.C., Mahaffy,J.M. and Zyskind,J.W. (2003) *Escherichia coli* cells with increased levels of DnaA and deficient in recombinational repair have decreased viability. *J. Bacteriol.*, **185**, 630–644.
77. Nordman,J., Skovgaard,O. and Wright,A. (2007) A novel class of mutations that affect DNA replication in *E. coli*. *Mol. Microbiol.*, **64**, 125–138.
78. Simmons,L.A., Breier,A.M., Cozzarelli,N.R. and Kaguni,J.M. (2004) Hyperinitiation of DNA replication in *Escherichia coli* leads to replication fork collapse and inviability. *Mol. Microbiol.*, **51**, 349–358.
79. Charbon,G., Bjorn,L., Mendoza-Chamizo,B., Frimodt-Moller,J. and Lobner-Olesen,A. (2014) Oxidative DNA damage is instrumental in hyperreplication stress-induced inviability of *Escherichia coli*. *Nucleic Acids Res.*, **42**, 13228–13241.
80. Guyer,M.S., Reed,R.R., Steitz,J.A. and Low,K.B. (1981) Identification of a sex-factor-affinity site in *E. coli* as gamma delta. *Cold Spring Harbor Symp. Quant. Biol.*, **45**, 135–140.
81. Jensen,K.F. (1993) The *Escherichia coli* K-12 "wild types" W3110 and MG1655 have an rph frameshift mutation that leads to pyrimidine starvation due to low pyrE expression levels. *J. Bacteriol.*, **175**, 3401–3407.
82. Howard-Flanders,P., Simson,E. and Theriot,L. (1964) A locus that controls filament formation and sensitivity to radiation in *Escherichia coli* K-12. *Genetics*, **49**, 237–246.
83. Singer,M., Baker,T.A., Schnitzler,G., Deischel,S.M., Goel,M., Dove,W., Jaacks,K.J., Grossman,A.D., Erickson,J.W. and Gross,C.A. (1989) A collection of strains containing genetically linked alternating antibiotic resistance elements for genetic mapping of *Escherichia coli*. *Microbiol. Rev.*, **53**, 1–24.
84. Lloyd,R.G. and Johnson,S. (1979) Kinetics of *recA* function in conjugational recombinant formation. *Mol. Gen. Genet.: MGG*, **169**, 219–228.
85. Leslie,N.R. and Sherratt,D.J. (1995) Site-specific recombination in the replication terminus region of *Escherichia coli*: functional replacement of dif. *EMBO J.*, **14**, 1561–1570.
86. Colloms,S.D., McCulloch,R., Grant,K., Neilson,L. and Sherratt,D.J. (1996) Xer-mediated site-specific recombination *in vitro*. *EMBO J.*, **15**, 1172–1181.
87. Blakely,G., May,G., McCulloch,R., Arciszewska,L.K., Burke,M., Lovett,S.T. and Sherratt,D.J. (1993) Two related recombinases are required for site-specific recombination at dif and cer in *E. coli* K12. *Cell*, **75**, 351–361.
88. Zyskind,J.W., Svitil,A.L., Stine,W.B., Biery,M.C. and Smith,D.W. (1992) RecA protein of Escherichia coli and chromosome partitioning. *Mol. Microbiol.*, **6**, 2525–2537.
89. Wardrope,L., Okely,E. and Leach,D. (2009) Resolution of joint molecules by RuvABC and RecG following cleavage of the *Escherichia coli* chromosome by EcoKI. *PLoS One*, **4**, e6542.